

Bis(Dithiolene)molybdenum Analogues Relevant to the DMSO Reductase Enzyme Family: Synthesis, Structures, and Oxygen Atom Transfer Reactions and Kinetics

Booyong Shim Lim and R. H. Holm*

Contribution from the Department of Chemistry and Chemical Biology, Harvard University, Cambridge, Massachusetts 02138

Received September 29, 2000

Abstract: A series of dithiolene complexes of the general type $[\text{Mo}^{\text{IV}}(\text{QR}')(\text{S}_2\text{C}_2\text{Me}_2)_2]^{1-}$ has been prepared and structurally characterized as possible structural and reactivity analogues of reduced sites of the enzymes DMSOR and TMAOR ($\text{QR}' = \text{PhO}^-$, 2-AdO⁻, PrⁱO⁻), dissimilatory nitrate reductase ($\text{QR}' = 2\text{-AdS}^-$), and formate dehydrogenase ($\text{QR}' = 2\text{-AdSe}^-$). The complexes are square pyramidal with the molybdenum atom positioned 0.74–0.80 Å above the S₄ mean plane toward axial ligand QR'. In part on the basis of a recent clarification of the active site of oxidized *Rhodobacter sphaeroides* DMSOR (Li, H.-K.; Temple, C.; Rajagopalan, K. V.; Schindelin, H. *J. Am. Chem. Soc.* 2000, 122, 7673), we have adopted the minimal reaction paradigm $\text{Mo}^{\text{IV}} + \text{XO} \rightleftharpoons \text{Mo}^{\text{VI}}\text{O} + \text{X}$ involving desoxo Mo(IV), monooxo Mo(VI), and substrate/product XO/X for direct oxygen atom transfer of DMSOR and TMAOR enzymes. The $[\text{Mo}(\text{OR}')(\text{S}_2\text{C}_2\text{Me}_2)_2]^{1-}$ species carry dithiolene and anionic oxygen ligands intended to simulate cofactor ligand and serinate binding in DMSOR and TMAOR catalytic sites. In systems with *N*-oxide and *S*-oxide substrates, the observed overall reaction sequence is $[\text{Mo}^{\text{IV}}(\text{OR}')(\text{S}_2\text{C}_2\text{Me}_2)_2]^{1-} + \text{XO} \rightarrow [\text{Mo}^{\text{VI}}\text{O}(\text{OR}')(\text{S}_2\text{C}_2\text{Me}_2)_2]^{1-} \rightarrow [\text{Mo}^{\text{VO}}(\text{S}_2\text{C}_2\text{Me}_2)_2]^{1-}$. Direct oxo transfer in the first step has been proven by isotope labeling. The reactivity of $[\text{Mo}(\text{OPh})(\text{S}_2\text{C}_2\text{Me}_2)_2]^{1-}$ (**1**) has been the most extensively studied. In second-order reactions, **1** reduces DMSO and (CH₂)₄SO ($k_2 \approx 10^{-6}$, $10^{-4} \text{ M}^{-1} \text{ s}^{-1}$; $\Delta S^\ddagger = -36$, -39 eu) and Me₃NO ($k_2 = 200 \text{ M}^{-1} \text{ s}^{-1}$; $\Delta S^\ddagger = -21 \text{ eu}$) in acetonitrile at 298 K. Activation entropies indicate an associative transition state, which from relative rates and substrate properties is inferred to be concerted with X–O bond weakening and Mo–O bond making. The Mo^{VI}O product in the first step, such as $[\text{Mo}^{\text{VI}}\text{O}(\text{OR}')(\text{S}_2\text{C}_2\text{Me}_2)_2]^{1-}$, is an intermediate in the overall reaction sequence, inasmuch as it is too unstable to isolate and decays by an internal redox process to a Mo^{VO} product, liberating an equimolar quantity of phenol. This research affords the first analogue reaction systems of biological *N*-oxide and *S*-oxide substrates that are based on desoxo Mo(IV) complexes with biologically relevant coordination. Oxo-transfer reactions in analogue systems are substantially slower than enzyme systems based on a $k_{\text{cat}}/K_{\text{M}}$ criterion. An interpretation of this behavior requires more information on the rate-limiting step(s) in enzyme catalytic cycles. (2-Ad = 2-adamantyl, DMSOR = dimethyl sulfoxide reductase, TMAOR = trimethylamine *N*-oxide reductase)

Introduction

It is now well-established that all known hydroxylase/oxotransferase molybdenum^{1–3} and tungsten⁴ enzymes contain mononuclear catalytic sites in which the metal atom is coordinated by one or two pterin-dithiolene cofactor ligands, as illustrated in Figure 1. The Hille classification of molybdoenzymes recognizes three major families.¹ Among them is the DMSO reductase (DMSOR) family, which includes DMSOR itself, trimethylamine *N*-oxide reductase (TMAOR), nitrate reductase, and formate dehydrogenase. (These and other abbreviations are listed in the Chart.) The increasing availability of structural results for catalytic sites in this family provides much of the information necessary for the formulation of

structural and functional synthetic analogues. The structures and reactivity of such analogues should be of considerable value in interpreting corresponding properties of enzyme sites. In this investigation, the enzymes of interest are DMSOR and TMAOR.

Crystal structures and molybdenum EXAFS results for *R*s^{5–8} and *R*c^{9–12} DMSOR, EXAFS data for *R*s biotin sulfoxide

- (1) Hille, R. *Chem. Rev.* **1996**, 96, 2757–2816.
- (2) Romão, M. J.; Knäblein, J.; Huber, R.; Moura, J. J. G. *Prog. Biophys. Mol. Biol.* **1997**, 68, 121–144.
- (3) Kisker, C.; Schindelin, H.; Rees, D. C. *Annu. Rev. Biochem.* **1997**, 66, 233–267.
- (4) Johnson, M. K.; Rees, D. C.; Adams, M. W. W. *Chem. Rev.* **1996**, 96, 2817–2839.

- (5) Schindelin, H.; Kisker, C.; Hilton, J.; Rajagopalan, K. V.; Rees, D. C. *Science* **1996**, 272, 1615–1621.
- (6) Li, H.-K.; Temple, C.; Rajagopalan, K. V.; Schindelin, H. *J. Am. Chem. Soc.* **2000**, 122, 7673–7680.
- (7) George, G. N.; Hilton, J.; Rajagopalan, K. V. *J. Am. Chem. Soc.* **1996**, 118, 1113–1117.
- (8) George, G. N.; Hilton, J.; Temple, C.; Prince, R. C.; Rajagopalan, K. V. *J. Am. Chem. Soc.* **1999**, 121, 1256–1266.
- (9) Schneider, F.; Löwe, J.; Huber, R.; Schindelin, H.; Kisker, C.; Knäblein, J. *J. Mol. Biol.* **1996**, 263, 53–69.
- (10) McAlpine, A. S.; McEwan, A. G.; Shaw, A. L.; Bailey, S. *J. Biol. Inorg. Chem.* **1997**, 2, 690–701.
- (11) McAlpine, A. S.; McEwan, A. G.; Bailey, S. *J. Mol. Biol.* **1998**, 275, 613–623.
- (12) Baugh, P. E.; Garner, C. D.; Charnock, J. M.; Collison, D.; Davies, E. S.; McAlpine, A. S.; Bailey, S.; Lane, I.; Hanson, G. R.; McEwan, A. G. *J. Biol. Inorg. Chem.* **1997**, 2, 634–643.

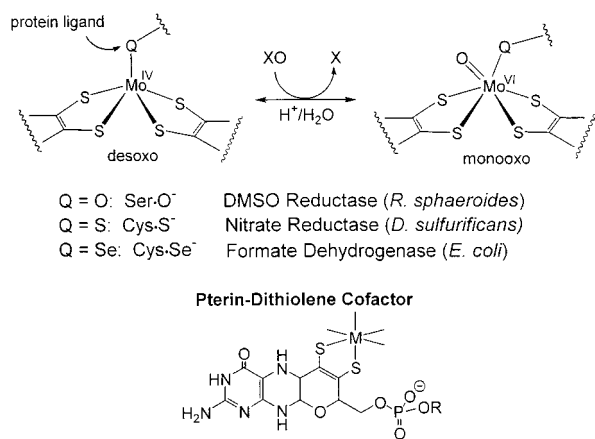


Figure 1. Depictions of simplified active-site structures of enzymes in the DMSOR family and the structure of the pterin-dithiolene cofactor (R absent or a nucleotide). Examples cited are crystallographic results (see text); the oxo ligand may be protonated in certain cases. EXAFS analyses indicate a selenosulfide-thiolate ligand in two FDH enzymes (not shown).

Chart 1. Designation of Complexes and Abbreviations

| | |
|---|------------------|
| $[\text{Mo}^{\text{IV}}(\text{O}^{\text{Ph}})(\text{S}_2\text{C}_2\text{Me}_2)_2]^{1-}$ | 1 ¹⁷ |
| $[\text{Mo}^{\text{IV}}(\text{O}^{\text{Ph}})(\text{S}_2\text{C}_2\text{Ph}_2)_2]^{1-}$ | 2 |
| $[\text{Mo}^{\text{IV}}(\text{OC}_6\text{F}_5)(\text{S}_2\text{C}_2\text{Me}_2)_2]^{1-}$ | 3 |
| $[\text{Mo}^{\text{IV}}(\text{OPr}^t)(\text{S}_2\text{C}_2\text{Me}_2)_2]^{1-}$ | 4 |
| $[\text{Mo}^{\text{IV}}(2\text{-AdO})(\text{S}_2\text{C}_2\text{Me}_2)_2]^{1-}$ | 5 ²² |
| $[\text{Mo}^{\text{IV}}(2\text{-AdS})(\text{S}_2\text{C}_2\text{Me}_2)_2]^{1-}$ | 6 ²² |
| $[\text{Mo}^{\text{IV}}(2\text{-AdSe})(\text{S}_2\text{C}_2\text{Me}_2)_2]^{1-}$ | 7 ²² |
| $[\text{Mo}^{\text{VI}}\text{O}(\text{O}^{\text{Ph}})(\text{S}_2\text{C}_2\text{Me}_2)_2]^{1-}$ | 8 |
| $[\text{Mo}^{\text{VO}}(\text{S}_2\text{C}_2\text{Me}_2)_2]^{1-}$ | 9 ²¹ |
| $[\text{Mo}^{\text{VO}}(\text{S}_2\text{C}_2\text{Ph}_2)_2]^{1-}$ | 10 |
| $[\text{Mo}^{\text{IV}}\text{O}(\text{S}_2\text{C}_2\text{Me}_2)_2]^{2-}$ | 11 ²¹ |

| | |
|-----------------------------------|---|
| 2-Ad | 2-adamantyl |
| bdt | benzene-1,2-dithiolate(2-) |
| Bu ^t L-NS ₂ | bis(4- <i>tert</i> -butylphenyl)-2-pyridylmethanethiolate(1-) |
| DMSOR | dimethylsulfoxide reductase |
| <i>Rc</i> | <i>Rhodobacter capsulatus</i> |
| <i>Rs</i> | <i>Rhodobacter sphaeroides</i> |
| S ₂ pd | pterin-dithiolene cofactor ligand |
| <i>Sm</i> | <i>Shewanella massilia</i> |
| TMAOR | trimethylamine N-oxide reductase |
| TMSO | tetramethylene S-oxide |
| X | generalized reduced product |
| XO | generalized oxidized substrate |

reductase,¹³ and a crystal structure of *Sm* TMAOR¹⁴ have been reported. The structure of oxidized *Rs* DMSOR at 1.3 Å recently determined by Li et al.⁶ clarifies an earlier structure at lower resolution (2.2 Å⁵) by showing that the enzyme as crystallized contains a disordered mixture of two types of sites: square pyramidal dioxo $[\text{Mo}^{\text{VI}}\text{O}_2(\text{O}\cdot\text{Ser})(\text{S}_2\text{pd})]$ and distorted trigonal prismatic monooxo $[\text{Mo}^{\text{VI}}\text{O}(\text{O}\cdot\text{Ser})(\text{S}_2\text{pd})_2]$. The latter is the probable catalytic site. In the fully reduced enzymes, X-ray and EXAFS data are consistent with the minimal formulation desoxo $[\text{Mo}^{\text{IV}}(\text{O}\cdot\text{Ser})(\text{S}_2\text{pd})_2]$ with possible additional coordination by water or hydroxide. Crystallography has identified the oxygen

ligand at ~1.9 Å as Ser147. Possibly the same type of disorder exists in the highly homologous *Rc* DMSOR, which has been described as having a seven-coordinate dioxo site when oxidized and a six-coordinate monooxo site when reduced,^{10–12} and in *Sm* TMAOR, but the matter has not been clarified.

Presented in Figure 1 are schematic minimal formulations of the oxidized and reduced sites of three enzymes in the DMSOR family for which structural information is available. In doing so, we adopt the six-coordinate structure of *Rs* DMSOR, assume the indicated reduced site for dissimilatory nitrate reductase, and do not include the selenosulfide-thiolate ligand form proposed on the basis of EXAFS analysis of two formate dehydrogenases.^{15,16} We take as the minimal reaction paradigm for direct oxygen atom transfer $\text{Mo}^{\text{IV}} + \text{XO} \rightleftharpoons \text{Mo}^{\text{VI}}\text{O} + \text{X}$,¹⁷ involving desoxo Mo(IV) and monooxo Mo(VI). Direct oxo transfer has been demonstrated for *Rs* DMSOR by ¹⁸O labeling,¹⁸ and, on the basis of results that follow, is highly probable for TMAOR. Recent research has resulted in the synthesis of bis(dithiolene)Mo(IV,VI) complexes of the desired structural types.^{17,19–21} Oxo-transfer reactivity of $[\text{Mo}^{\text{IV}}(\text{OSiBu}^t\text{Ph}_2)(\text{bdt})_2]^{1-}$ with sulfoxides is sluggish and incomplete, even at 50 °C, and with Me₃NO, some conversion to $[\text{Mo}^{\text{VI}}\text{O}(\text{OSiBu}^t\text{Ph}_2)(\text{bdt})_2]^{1-}$ occurs, but the reaction is not clean.¹⁹ Also, this complex is not reduced by sulfides. To provide an electronic environment more closely related to that apparently present at DMSOR and TMAOR catalytic sites, we have turned to complexes that are derived from the dialkyl-dithiolene 1,2-Me₂C₂S₂²⁻. In this work, we describe the synthesis and structures of $[\text{Mo}(\text{QR})(\text{S}_2\text{C}_2\text{Me}_2)_2]^{1-}$ (Q = O, S, Se), intended as analogues of desoxo Mo(IV) sites in the DMSOR family (Figure 1), and the oxo-transfer reactivity of complexes with axial anionic oxygen ligands. Elsewhere, we have reported molybdenum K-edge spectra and EXAFS of these complexes in order to facilitate site identification by X-ray absorption spectroscopy.²²

In view of the existence of molybdenum and tungsten iso-enzymes,^{23,24} we have endeavored to develop tungsten dithiolene chemistry^{17,25–27} in parallel with that of molybdenum dithiolenes. The oxo-transfer reactivity of the related tungsten com-

(13) Temple, C. A.; George, G. N.; Hilton, J. C.; George, M. G.; Prince, R. C.; Barber, M. J.; Rajagopalan, K. V. *Biochemistry* **2000**, *39*, 4046–4052.

(14) Czjzek, M.; Dos Santos, J.-P.; Pommier, J.; Giordano, G.; Méjean, V.; Haser, R. *J. Mol. Biol.* **1999**, *284*, 435–447.

(15) George, G. N.; Colangelo, C. M.; Dong, J.; Scott, R. A.; Khangulov, S. V.; Gladyshev, V. N.; Stadtman, T. C. *J. Am. Chem. Soc.* **1998**, *120*, 0, 1267–1273.

(16) George, G. N.; Costa, C.; Moura, J. J. G.; Moura, I. *J. Am. Chem. Soc.* **1999**, *121*, 2625–2626.

(17) Lim, B. S.; Sung, K.-M.; Holm, R. H. *J. Am. Chem. Soc.* **2000**, *122*, 7410–7411.

(18) Schultz, B. E.; Holm, R. H.; Hille, R. *J. Am. Chem. Soc.* **1995**, *117*, 827–828.

(19) Donahue, J. P.; Goldsmith, C. R.; Nadiminti, U.; Holm, R. H. *J. Am. Chem. Soc.* **1998**, *120*, 12869–12881.

(20) Musgrave, K. B.; Donahue, J. P.; Lorber, C.; Holm, R. H.; Hedman, B.; Hodgson, K. O. *J. Am. Chem. Soc.* **1999**, *121*, 10297–10307.

(21) Lim, B. S.; Donahue, J. P.; Holm, R. H. *Inorg. Chem.* **2000**, *39*, 263–273.

(22) Musgrave, K. B.; Lim, B. S.; Sung, K.-M.; Holm, R. H.; Hedman, B.; Hodgson, K. O. *Inorg. Chem.* **2000**, *39*, 5238–5247.

(23) Buc, J.; Santini, C.-L.; Giordano, R.; Czjzek, M.; Giordano, G. *Mol. Microbiol.* **1999**, *32*, 159–168.

(24) Stewart, L. J.; Bailey, S.; Bennett, B.; Charnock, J. M.; Garner, C. D.; McAlpine, A. S. *J. Mol. Biol.* **2000**, *299*, 593–600.

(25) Lorber, C.; Donahue, J. P.; Goddard, C. A.; Nordlander, E.; Holm, R. H. *J. Am. Chem. Soc.* **1998**, *120*, 8112.

(26) Goddard, C. A.; Holm, R. H. *Inorg. Chem.* **1999**, *38*, 5389–5398.

(27) (a) Sung, K.-M.; Holm, R. H. *Inorg. Chem.* **2000**, *39*, 1275–1281.

(b) Sung, K.-M.; Holm, R. H. *J. Am. Chem. Soc.* **2001**, *123*, 1931–1943.

plexes $[\text{W}(\text{OR})(\text{S}_2\text{C}_2\text{Me}_2)_2]^{-1}$ and their comparison to molybdenum dithiolenes is described in a separate report.^{27b}

Experimental Section

Preparation of Compounds. All reactions and manipulations were conducted under a pure dinitrogen atmosphere using either an inert atmosphere box or standard Schlenk techniques. Acetonitrile and dichloromethane were freshly distilled from CaH_2 , and methanol was distilled from magnesium; CD_3CN , $\text{THF-}d_8$, and Me_2SO (Aldrich) were dried over freshly activated molecular sieves. Ether and THF were distilled from sodium/benzophenone and stored over 4 Å molecular sieves. Tetramethylenesulfoxide (Fluka) was distilled from CaH_2 under reduced pressure before use. In the following preparations, all volume reduction and evaporation steps were performed in vacuo. The compounds NaOPh , $(\text{Et}_4\text{N})(\text{OC}_6\text{F}_5)$, LiOPr^i , $\text{Li}(2\text{-AdO})$, and $\text{Li}(2\text{-AdS})$ were prepared from the corresponding phenol, alcohol, thiol, or selenol using NaOMe , Et_4NOH (25% in MeOH), or Bu^nLi (1.6 M in hexane). The compound 2-AdSH was obtained by a published method.²⁸ Elemental selenium was obtained from Lancaster.

Bi(2-adamantyl)diselenide. To a mixture of 2-bromoadamantane (5.00 g, 0.023 mol) and Mg (9.00 g, 0.37 mol) was added 250 mL of ether. The reaction was initiated by adding 0.1 mL of 1,2-dibromothane. The reaction mixture was refluxed overnight (without mechanical stirring to avoid formation of 2,2'-biadamantane²⁹), filtered, and the filtrate was introduced into a flask containing selenium powder (1.8 g, 0.023 mol). THF (50 mL) was added, and the mixture was stirred overnight. The pale yellow solution was opened to the air, stirred for another 6 h, and filtered. The filtrate was reduced to dryness to give a yellow solid, which was dissolved in a minimal volume of hexanes and chromatographed on silica gel with ether in pentane (0–2%). The product was obtained as a yellow powder (3.5 g, 71%) after removal of solvents: mp 215–217 °C. ^{13}C NMR (CDCl_3): 27.3, 27.9, 32.6, 34.0, 37.7, 39.2, 56.7. ^1H NMR (CDCl_3): δ 1.56–2.19 (m, 28), 3.64 (s, 2). EI-MS⁺: 430 (M^+).

$(\text{Et}_4\text{N})[\text{Mo}(\text{OPh})(\text{S}_2\text{C}_2\text{Me}_2)_2]$. A suspension of NaOPh (24 mg, 0.21 mmol) in 2 mL of acetonitrile was added to a suspension of $[\text{Mo}(\text{CO})_2(\text{S}_2\text{C}_2\text{Me}_2)_2]^{21}$ (54 mg, 0.20 mmol) in 2 mL of acetonitrile. The mixture was stirred for 6 h to generate a brown solution. A solution of Et_4NCl (34 mg, 0.21 mmol) in 1 mL of acetonitrile was added. The mixture was stirred for 10 min and filtered. The filtrate was reduced to one-third of its original volume, several volume equivalents of ether were layered onto the solution, and the mixture was allowed to stand for 2 days. The product was obtained as black bar-type crystals (54 mg, 48%). ^1H NMR (anion, CD_3CN): δ 2.54 (s, 12), 6.38 (d, 2), 6.78–(t, 1), 7.01 (m, 2). Absorption spectrum (acetonitrile): λ_{nm} (ϵ_{M}) 275 (sh, 10900), 345 (12300), 395 (4100), 478 (1790), 565 (sh, 750), 730 (728) nm. Anal. Calcd. for $\text{C}_{32}\text{H}_{37}\text{MoNOS}_4$: C, 47.55; H, 6.71; N, 2.52; S, 23.08. Found: C, 47.48; H, 6.72; N, 2.50; S, 23.15.

$(\text{Et}_4\text{N})[\text{Mo}(\text{OPh})(\text{S}_2\text{C}_2\text{Ph}_2)_2]$. The preceding method was followed but with use of $[\text{Mo}(\text{CO})_2(\text{S}_2\text{C}_2\text{Ph}_2)_2]^{21}$. The product was obtained as dark brown crystals (48%). ^1H NMR (anion, CD_3CN): δ 6.54 (m, 2), 6.83 (m, 1), 7.05 (m, 2), 7.19–7.38 (m, 20). Absorption spectrum (acetonitrile): λ_{max} (ϵ_{M}) 320 (22700), 349 (29000), 400 (sh, 6470), 470 (sh, 2300), 560 (798), 690 (428) nm. Anal. Calcd. for $\text{C}_{42}\text{H}_{45}\text{MoNOS}_4$: C, 62.73; H, 5.64; N, 1.74; S, 15.95. Found: C, 62.65; H, 5.71; N, 1.68; S, 15.97.

$(\text{Et}_4\text{N})[\text{Mo}(\text{OC}_6\text{F}_5)(\text{S}_2\text{C}_2\text{Me}_2)_2]$. A solution of $(\text{Et}_4\text{N})(\text{OC}_6\text{F}_5)$ (80 mg, 0.26 mmol) in 1 mL of THF was filtered through Celite and added to a solution of $[\text{Mo}(\text{CO})_2(\text{S}_2\text{C}_2\text{Me}_2)_2]$ (100 mg, 0.26 mmol) in 2 mL of THF. The reaction mixture was stirred for 6 h to generate a brown precipitate. This material was collected by filtration and washed with $\text{THF}(1 \times 1 \text{ mL})$ and $\text{Et}_2\text{O}(2 \times 2 \text{ mL})$ to afford the product as a brown solid (75 mg, 45%). ^1H NMR (anion, $\text{THF-}d_8$): δ 2.57 (s, 12). ^{19}F NMR ($\text{THF-}d_8$, $\text{BF}_3\text{Et}_2\text{O}$ reference): δ -161 (d, 2), -170 (t, 2), -175 (t, 1). Absorption spectrum (THF): λ_{max} (ϵ_{M}) 358 (10700), 425 (4060), 502 (sh, 1610), 594 (sh, 735), 740 (262) nm. Anal. Calcd. for $\text{C}_{22}\text{H}_{32}\text{F}_5\text{-}$

MoNOS_4 : C, 40.92; H, 5.00; N, 2.17; S, 19.86. Found: C, 40.78; H, 5.10; N, 2.26; S, 19.91.

$(\text{Et}_4\text{N})[\text{MoO}(\text{S}_2\text{C}_2\text{Ph}_2)_2]$. This compound was prepared by the oxidation of $(\text{Et}_4\text{N})_2[\text{MoO}(\text{S}_2\text{C}_2\text{Ph}_2)_2]$ with iodine in a procedure analogous to that for $(\text{Et}_4\text{N})[\text{MoO}(\text{S}_2\text{C}_2\text{Me}_2)_2]$.²¹ The product was isolated as black crystals (50%). IR (KBr): ν_{MoO} 926 cm^{-1} . Absorption spectrum (acetonitrile): λ_{max} (ϵ_{M}) 600 (sh, 715), 867 (3770) nm. Anal. Calcd. for $\text{C}_{36}\text{H}_{40}\text{MoNOS}_4$: C, 59.48; H, 5.55; N, 1.93; S, 17.64. Found: C, 59.39; H, 5.62; N, 1.87; S, 17.55.

$(\text{Et}_4\text{N})[\text{Mo}(\text{OPr}^i)(\text{S}_2\text{C}_2\text{Me}_2)_2]$. A solution of LiOPr^i (22 mg, 0.33 mmol) in 1 mL of THF was added to a suspension of $[\text{Mo}(\text{CO})_2(\text{S}_2\text{C}_2\text{Me}_2)_2]$ (125 mg, 0.32 mmol) in 2 mL of acetonitrile. The reaction mixture was stirred overnight to produce a brown solution. A solution of Et_4NCl (55 mg, 0.33 mmol) in 1 mL of acetonitrile was added. The mixture was stirred for 10 min and filtered; the filtrate was reduced to dryness. The black solid residue was dissolved in a minimal volume of acetonitrile. Several volume equivalents of ether were layered onto the solution, and the mixture was allowed to stand for 2 days. The product was isolated as a brown microcrystalline solid (85 mg, 51%). ^1H NMR (anion, CD_3CN): δ 0.84 (d, 6), 2.48 (s, 12), 3.73 (m, 1). Absorption spectrum (acetonitrile): λ_{max} (ϵ_{M}) 264 (703), 325 (9980), 378 (4570), 460 (1380), 630 (sh, 305) nm. Anal. Calcd. for $\text{C}_{19}\text{H}_{39}\text{MoNOS}_4$: C, 43.74; H, 7.53; N, 2.68; S, 24.58. Found: C, 43.66; H, 7.46; N, 2.64; S, 24.65.

$(\text{Et}_4\text{N})[\text{Mo}(2\text{-AdO})(\text{S}_2\text{C}_2\text{Me}_2)_2]$. A solution of $\text{Li}(2\text{-AdO})$ (26 mg, 0.16 mmol) in 1 mL of THF was added to a solution of $[\text{Mo}(\text{CO})_2(\text{S}_2\text{C}_2\text{Me}_2)_2]$ (64 mg, 0.16 mmol) in 2 mL of THF. The reaction mixture was stirred overnight. To the brown solution was added a solution of Et_4NCl (27 mg, 0.16 mmol) in 2 mL of acetonitrile. The mixture was stirred for 10 min; solvent was removed to give a black solid. The solid was then dissolved in a minimal volume of THF and several volume equivalents of ether were added. Large black needlelike crystals of the product were collected, washed with ether, and dried (65 mg, 65%). ^1H NMR (anion, CD_3CN): δ 1.18–1.21 (d, br, 2), 1.44–1.70 (m, br, 12), 2.46 (s, 12), 3.55 (t, br, 1). Absorption spectrum (acetonitrile): λ_{nm} (ϵ_{M}) 264 (8340), 327 (9000), 373 (3970), 453 (sh, 1690), 528 (sh, 864), 850 (sh, 389) nm. Anal. Calcd. for $\text{C}_{26}\text{H}_{47}\text{MoNOS}_4$: C, 50.87; H, 7.72; N, 2.28; S, 20.89. Found: C, 50.84; H, 7.79; N, 2.30; S, 20.73.

$(\text{Et}_4\text{N})[\text{Mo}(2\text{-AdS})(\text{S}_2\text{C}_2\text{Me}_2)_2]$. A solution of $\text{Li}(2\text{-AdS})$ (38 mg, 0.22 mmol) in 1 mL of THF was added to a suspension of $[\text{Mo}(\text{CO})_2(\text{S}_2\text{C}_2\text{Me}_2)_2]$ (84 mg, 0.22 mmol) in 2 mL of acetonitrile. Upon stirring, the solution became brown-green; the reaction mixture was stirred for 3 h. To the mixture was added a solution of Et_4NCl (36 mg, 0.22 mmol) in 2 mL of acetonitrile; stirring was continued for 10 min to give a brown-green solution. Solvents were removed, leaving a red-brown solid, which was dissolved in a minimal volume of acetonitrile. Several volume equivalents of ether were introduced by vapor diffusion. The product separated as black blocklike crystals (70 mg, 51%). ^1H NMR (anion, CD_3CN): δ 1.22–1.79 (m, br, 14), 2.74 (s, 12), 2.82 (s, br, 1). Absorption spectrum (acetonitrile): λ_{max} (ϵ_{M}) 278 (9030), 342 (15800), 447 (3610), 528 (sh, 1900) nm. Anal. Calcd. for $\text{C}_{26}\text{H}_{47}\text{MoNS}_4$: C, 49.57; H, 7.52; N, 2.22; S, 25.45. Found: C, 49.64; H, 7.63; N, 2.26; S, 25.54.

$(\text{Et}_4\text{N})[\text{Mo}(2\text{-AdSe})(\text{S}_2\text{C}_2\text{Me}_2)_2]$. The preceding method was followed but with use of 2-AdSe⁻ anion generated in situ by treating (2-AdSe)₂ with LiBHEt_3 (1 M in THF). The brown-green reaction solution was reduced to dryness, and the solid residue was redissolved in 5 mL of acetonitrile. The solvent was removed slowly in vacuo. This procedure was repeated 10 times. The final solid material was washed with acetonitrile ($2 \times 2 \text{ mL}$) to obtain a red-brown solid. The filtrate was subject to the same procedure to afford additional red-brown solid. (These tedious dissolution/solvent removal steps are required to promote the removal of carbonyl groups from the starting material.) The combined solids were dissolved in a minimal volume of acetonitrile to generate a bright red-brown solution, which was filtered through Celite. Several volume equivalents of ether were added to the filtrate. After several days, the product was obtained as black needlelike crystals (30%). ^1H NMR (anion, CD_3CN): δ 1.34–1.81 (m, br, 14), 2.79 (s, 12), 3.29 (s, br, 1). Absorption spectrum (acetonitrile): λ_{max} (ϵ_{M}) 293 (6730), 351 (15600), 396 (sh, 5570), 463 (sh, 2900), 530 (sh, 1640), 750 (sh,

(28) Greidanus, J. W. *Can. J. Chem.* **1970**, *48*, 3593–3597.

(29) Molle, G.; Bauer, P.; Dubois, J. E. *J. Org. Chem.* **1982**, *47*, 4120–4128.

Table 1. Crystallographic Data^a for Compounds Containing 2–7

| | (Et ₄ N)[2]·0.5MeCN | (Et ₄ N)[3]·THF | (Et ₄ N)[4] | (Et ₄ N)[5] | (Et ₄ N)[6]·0.3Et ₂ O | (Et ₄ N)[7]·0.3Et ₂ O |
|---|--|---|--|--|--|---|
| formula | C ₄₃ H _{46.5} MoN _{1.5} OS ₄ | C ₂₆ H ₄₀ F ₅ MoNO ₂ S ₄ | C ₁₉ H ₃₉ MoNOS ₄ | C ₂₆ H ₄₇ MoNOS ₄ | C _{27.2} H ₅₀ MoNO _{0.3} S ₅ | C _{27.5} H ₅₀ MoNO _{0.3} S ₄ Se |
| fw | 824.50 | 717.77 | 521.69 | 613.87 | 652.12 | 699.02 |
| crystal system | monoclinic | triclinic | triclinic | orthorhombic | orthorhombic | orthorhombic |
| space group | <i>Cc</i> | <i>P</i> $\bar{1}$ | <i>P</i> $\bar{1}$ | <i>Pnma</i> | <i>I4(1)/a</i> | <i>I4(1)/a</i> |
| Z | 8 | 2 | 2 | 4 | 16 | 16 |
| <i>a</i> , Å | 44.188(4) | 9.2550(9) | 9.3067(9) | 23.9500(6) | 36.233(2) | 36.413(2) |
| <i>b</i> , Å | 9.8658(8) | 13.295(1) | 11.514(1) | 11.4467(3) | 36.233(2) | 36.413(2) |
| <i>c</i> , Å | 19.673(2) | 13.569(1) | 12.674(1) | 11.1152(3) | 9.8980(6) | 9.7755(6) |
| α , deg | | 79.465(2) | 87.551(2) | | | |
| β , deg | 99.032(2) | 81.938(2) | 76.498(2) | | | |
| γ , deg | | 78.231(2) | 71.353(2) | | | |
| <i>V</i> , Å ³ | 8470(1) | 1597.6(3) | 1250.5(2) | 3047.2(1) | 12995(1) | 12961(1) |
| <i>d</i> _{calc} , g/cm ³ | 1.293 | 1.492 | 1.386 | 1.338 | 1.333 | 1.433 |
| μ , mm ⁻¹ | 0.540 | 0.725 | 0.867 | 0.723 | 0.743 | 1.808 |
| θ range, deg | 1.87–28.30 | 1.54–22.50 | 1.65–28.32 | 1.70–25.00 | 1.12–28.31 | 1.12–22.49 |
| GOF(<i>F</i> ²) | 1.037 | 1.087 | 1.003 | 1.053 | 1.078 | 1.069 |
| <i>R</i> ₁ ^b (<i>wR</i> ₂ ^c), % | 4.23(8.86) | 3.79(9.73) | 3.49(8.01) | 3.61(9.47) | 4.34(9.99) | 2.94(7.53) |

^a Obtained with graphite monochromated Mo K α ($\lambda = 0.71073$ Å) radiation. ^b $R_1 = \sum |F_o| - |F_d| / \sum |F_o|$. ^c $wR_2 = \{\sum [w(F_o^2 - F_c^2)^2] / \sum [w(F_o^2)^2]\}^{1/2}$.

69) nm. Anal. Calcd. for C₂₆H₄₇MoNS₄Se: C, 46.14; H, 7.00; N, 2.07; S, 18.95; Se, 11.67. Found: C, 46.21; H, 7.01; N, 2.13; S, 19.08; Se, 11.56.

2-Thiaindane S-oxide-[¹⁸O]. This compound was prepared in a manner similar to described procedures.^{30,31} A solution of bromine (0.52 mL, 0.01 mol) was added to a solution of 2-thiaindane³² (1.36 g, 0.01 mol) in 100 mL of hexane with stirring. Immediately, yellow 2-thiaindane S-dibromide formed and was collected by filtration. The dibromide was added in small portions with stirring to a mixture of freshly distilled triethylamine (1.40 mL, 0.01 mol) and H₂[¹⁸O] (95%, 0.25 mL, 0.012 mol) in 100 mL of dichloromethane. The yellow color bleached as the reaction proceeded. After stirring for 3 h, the reaction mixture was filtered, and the filtrate was reduced to dryness. The residue was twice flash-chromatographed on silica gel with ethyl acetate in hexane (0–90%). Removal of solvent afforded the product as 0.50 g (32%) of off-white solid. IR (KBr): ν (S[¹⁸O]) 998 cm⁻¹, ν (S[¹⁶O]) 1035 cm⁻¹. ¹H NMR (CDCl₃): δ 4.05(d, 2), 4.21(d, 2), 7.24–7.31(m, 4). EI–CI mass spectrometry showed the product to contain 82% ¹⁸O.

¹⁸O Transfer Reactions. (a) with Ph₂Se[¹⁸O]. (Et₄N)[Mo(OPh)-(S₂C₂Me₂)₂] (7.6 mg, 13.7 mmol) and Ph₂Se[¹⁸O] (62%)²⁵ (4.55 mg, 18.1 mmol) were stirred in 1 mL of acetonitrile for 3 h. The solvent was removed in vacuo, and the residue was washed with ether (5 × 2 mL). IR (KBr): ν (Mo[¹⁸O]) 874 cm⁻¹, ν (Mo[¹⁶O]) 917 cm⁻¹. FAB-MS: ¹⁸O product incorporation 37%. **(b) with C₆H₄(CH₂)₂S[¹⁸O].** (Et₄N)[Mo(OPh)(S₂C₂Me₂)₂] (2.35 mg, 4.23 mmol) and C₆H₄(CH₂)₂S[¹⁸O] (82%) (55.0 mg, 0.357 mmol) were stirred in 1 mL of acetonitrile over 2 days at 50 °C. The solvent was removed in vacuo, and the residue was washed with ether (5 × 5 mL). IR(KBr): ν (Mo[¹⁸O]) 875 cm⁻¹. FAB-MS: ¹⁸O product incorporation 30%.

Reactions of CO with (Et₄N)[Mo(2-AdQ)(S₂C₂Me₂)₂] (Q = O, S, Se). Carbon monoxide was bubbled through a solution of (Et₄N)[Mo(2-AdQ)(S₂C₂Me₂)₂] (Q = O, 3.40 mM; Q = S, 1.80 mM; Q = Se, 5.39 mM) for 20 min. IR spectra of the resulting solutions showed ν_{CO} at 1955, 1944, and 1952 cm⁻¹ for Q = O, S, and Se, respectively. Absorption spectra were subsequently measured.

Detection of Tetrahydrothiophene. A mixture of (Et₄N)[Mo(OPh)-(S₂C₂Me₂)₂] (800 μ L, 2.30 mM), tetramethylenesulfoxide (80 μ L, 1.01 M), and toluene (1 μ L, internal reference) was stirred at 50 °C for 8 h. A small proton (1 μ L) of the resulting solution was injected for gas chromatography, and the peak profiles were analyzed by comparison with those of authentic tetramethylenesulfoxide and tetrahydrothiophene at the same temperature gradients (50–150 °C for 25 min). A mixture of acetonitrile (800 μ L), tetramethylenesulfoxide (80 μ L), and toluene (1 μ L) without (Et₄N)[Mo(OPh)(S₂C₂Me₂)₂] that was treated in the same way as the above mixture showed no peak corresponding to tetrahydrothiophene.

(30) Drabowicz, J.; Midura, W.; Mikolajczyk, M. *Synthesis* **1979**, 39–40.

(31) Kreher, R. P.; Kalischko, J. *Chem. Ber.* **1991**, *124*, 645–654.

(32) Holland, H. L.; Turner, C. D.; Andreana, P. R.; Nguyen, D. *Can. J. Chem.* **1999**, *77*, 463–471.

Kinetics Measurements. Sample preparations and reactions were performed under strictly anaerobic conditions in acetonitrile or THF solutions. Reactions were monitored spectrophotometrically with a Cary 3 instrument equipped with a cell compartment thermostated to ± 0.5 °C. S-oxide substrate reduction reactions were followed by observing the appearance of the 830-nm band of [Mo^{VO}(S₂C₂Me₂)₂]¹⁻ except for the [Mo(OPh)(S₂C₂Ph₂)₂]¹⁻ system, in which disappearance of the 349-nm band of this complex was monitored. N-oxide substrate reduction reactions were monitored by the appearance of the 610-nm band of [Mo^{VI}O(OPh)(S₂C₂Me₂)₂]¹⁻. Decreases in intensity of the 345- and 327-nm bands of [Mo(OPh)(S₂C₂Me₂)₂]¹⁻ and [Mo(OPr^t)(S₂C₂Me₂)₂]¹⁻, respectively, were followed for hydrolysis reactions. Sharp isobestic points demonstrated that these oxo-transfer reactions proceeded cleanly: [Mo(OPh)(S₂C₂Me₂)₂]¹⁻ → [MoO(OPh)(S₂C₂Me₂)₂]¹⁻ (372 nm), [MoO(S₂C₂Me₂)₂]¹⁻ (552 nm), [MoO(S₂C₂Me₂)₂]²⁻ (739 nm); [Mo(OPh)(S₂C₂Ph₂)₂]¹⁻ → [MoO(S₂C₂Ph₂)₂]¹⁻ (583 nm); [Mo(OC₆F₅)(S₂C₂Me₂)₂]¹⁻ → [MoO(S₂C₂Me₂)₂]¹⁻ (548 nm); [Mo(OPr^t)(S₂C₂Me₂)₂]¹⁻ → [MoO(S₂C₂Me₂)₂]¹⁻ (305, 532 nm), [MoO(S₂C₂Me₂)₂]²⁻ (299, 711 nm); [MoO(OPh)(S₂C₂Me₂)₂]¹⁻ → [MoO(S₂C₂Me₂)₂]¹⁻ (747 nm). Reaction systems contained the initial concentrations [[Mo(OR')(S₂C₂R₂)₂]¹⁻]₀ = 0.314–1.11 mM and excess substrate: [Me₂SO]₀ = 8.46–10.1 M, [(CH₂)₄SO]₀ = 0.218–1.53 M, [H₂O]₀ = 0.0914–0.261 M, [Me₃NO]₀ = 0.973–1.31 mM, [(C₆H₄CH₂)₃NO]₀ = 1.11–1.62 mM.

For each substrate, reactions were run at a minimum of four temperatures in the range of 288–338 K. At each temperature, at least four runs were performed under pseudo-first-order conditions for S-oxide reduction and hydrolysis reactions or under second-order conditions for N-oxide reduction reactions. Plots of ln[(A - A_∞)/(A₀ - A_∞)] vs time (S-oxide reductions and hydrolysis reactions) or ln[1 + {(N-oxide)₀ - [Mo]₀(A₀ - A_∞)} / [Mo]₀(A - A_∞)] vs time (N-oxide reductions) were linear over 3 half-lives. Linear plots of *k*_{obs} vs substrate concentration yielded the second-order rate constants, *k*₂, for S-oxide reduction and hydrolysis reactions. The second-order rate constants, *k*₂, for N-oxide reductions were determined as mean values from at least five independent measurements at different concentrations. These second-order rate constants, *k*₂, were used to determine activation parameters by means of Eyring plots. The first-order rate constant, *k*₁, for the reaction [MoO(OPh)(S₂C₂Me₂)₂]¹⁻ → [MoO(S₂C₂Me₂)₂]¹⁻ was obtained as a mean value of two independent measurements in the range [Mo^{VI}]₀ = 0.7–2.0 mM. Errors were estimated using linear least-squares error analysis with uniform weighting of the data points³³ or standard deviations.

In the sections that follow, molybdenum complexes are numerically designated following the Chart, which also includes abbreviations.

X-ray Structure Determinations. The six compounds listed in Table 1 were structurally characterized by X-ray crystallography. Crystals of (Et₄N)[3]·THF were grown from a saturated THF solution held at -25 °C for several days. All other crystals were obtained by

(33) Clifford, A. A. *Multivariate Error Analysis*; John Wiley & Sons: New York, 1973.

Table 2. Bond Distances (Å) and Angles (deg) for Complexes with Axial Oxygen Ligands

| | 1 ^a | 2 ^b | 3 | 4 | 5 |
|-------------------|----------------|----------------|----------|----------|-----------------------|
| Mo–O1 | 1.898(5) | 1.868(8) | 1.933(3) | 1.843(2) | 1.839(3) |
| Mo–S ^b | 2.32(5) | 2.31(1) | 2.309(1) | 2.325(8) | 2.333(6) |
| C–S ^b | 1.77(2) | 1.77(2) | 1.765(2) | 1.77(3) | 1.776(1) |
| C–C ^c | 1.330(5) | 1.35(3) | 1.322(3) | 1.321(6) | 1.330(1) |
| Mo–O1–C | 134.7(4) | 145(1) | 128.1(2) | 139.0(2) | 120.0(4) ^d |
| δ ^e | 0.795 | 0.798 | 0.752 | 0.783 | 0.762 |
| θ ^f | 125.7 | 125.5 | 128.3 | 126.7 | 128.6 |

^a Ref 10. ^b Mean values. ^c Chelate ring. ^d Values taken from the major occupancy of the disordered 2-adamantyl group. ^e Perpendicular displacement of Mo atom from S₄ least-squares plane. ^f Dihedral angle between MoS₂ planes.

vapor diffusion where the first component specified is the parent solvent: (Et₄N)[1], (Et₄N)[2]·0.5MeCN, (Et₄N)[4], (Et₄N)[6,7]·0.3Et₂O from acetonitrile/ether; (Et₄N)[5], from THF/ether. Crystals were mounted on glass capillary fibers in grease and cooled in a stream of dinitrogen (–60 °C). Diffraction data were obtained with a Siemens (Bruker) SMART CCD area detector system using ω scans of 0.3°/frame, 30-s frames such that 1271 frames were collected for a hemisphere of data. The first 50 frames were re-collected at the end of the data collections to monitor for crystal decay; no significant decay was observed. Cell parameters were determined using SMART software. Data reduction was performed with SAINT software, which corrects for Lorentz polarization and decay. Absorption corrections were applied by using the program SADABS. Space groups were assigned by analysis of symmetry and observed systematic absences determined by the program XPREP and by successful refinement of the structures. All of the structures were solved by direct methods with SHELXS and subsequently refined against all of the data by the standard technique of full-matrix least-squares on F² (SHELXL-97, SHELXL-93).

Asymmetric units contain one ((Et₄N)[3]·THF,[4],[6]·0.3Et₂O,[7]·0.3Et₂O)) or two ((Et₄N)[2]·0.5MeCN) formula weights, except for (Et₄N)[5], which contains one-half formula weight, owing to an imposed mirror plane. The structure of (Et₄N)[2]·0.5MeCN was refined as a racemic twin. Disordered atoms or groups were frequently found in the structures. The 2-adamantyl group of (Et₄N)[5] is disordered over three different positions, one of which is generated by the imposed mirror plane, and was refined with 0.5, 0.25, and 0.25 occupancy factors. The selenium atom in (Et₄N)[7]·0.3Et₂O is disordered over two sites and was refined with occupancy factor 0.92. The 2-adamantyl groups of (Et₄N)[6,7]·0.3Et₂O are disordered over two sites and were refined with occupancy factors 0.83 and 0.85, respectively. Methylene groups of the cations in (Et₄N)[4–7] are disordered over two sites and were refined with site occupancy factors of 0.72, 0.51, 0.64, and 0.63, respectively. The acetonitrile solvate molecule in (Et₄N)[2]·0.5MeCN and the THF solvate molecule in (Et₄N)[3]·THF were found to be disordered over two positions and were refined accordingly. Ether solvate molecules in (Et₄N)[6,7]·0.3Et₂O are found in a chainlike arrangement over the lattice and were treated isotropically. All non-hydrogen atoms other than in solvate molecules were described anisotropically. In the final stages of refinement, hydrogen atoms were added at idealized positions and refined as riding atoms with a uniform value of U_{iso}. Final refined structures were examined for any overlooked symmetry with the checking program PLATON. Crystallographic and final agreement factors are included in Table 1. Metric parameters for the structures are collected in Tables 2 and 3. Because of the large quantity of data, mean values are given where feasible instead of individual data. (See paragraph at the end of this article for available Supporting Information.)

Other Physical Measurements. Absorption spectra were recorded with a Varian Cary 50 Bio spectrophotometer. ¹H NMR spectra were obtained with Varian Mercury 400/500 spectrometers. Infrared spectra were measured with a Nicolet Nexus 470 Fourier transform IR instrument. EPR spectra were obtained with a Bruker ESP-300 spectrometer. Gas chromatographic analysis was performed with a Hewlett-Packard 5890 Series II gas chromatograph equipped with an HP-5 cross-linked 5% silicone column.

Table 3. Bond Distances (Å) and Angles (deg) for Complexes with Axial Thiolate and Selenolate Ligands

| | 6 | 7 |
|---------------------------|----------|----------|
| Mo–S5/Se1 ^a | 2.312(1) | 2.439(1) |
| Mo–S ^b | 2.315(3) | 2.317(3) |
| C–S ^b | 1.76(2) | 1.76(1) |
| C–C ^c | 1.32(1) | 1.324(1) |
| Mo–S5/Se1–C9 ^a | 101.4(4) | 102.5(1) |
| δ ^d | 0.746 | 0.740 |
| θ ^e | 129.4 | 129.8 |

^a Values taken from the major occupancy. ^b Mean values. ^c Chelate ring. ^d Perpendicular displacement of Mo atom from S₄ least-squares plane. ^e Dihedral angle between MoS₂ planes.

Results and Discussion

Synthesis and Structures of Compounds. As shown previously, the complexes [Mo(CO)₂(S₂C₂R₂)₂] (R = Me, Ph) readily undergo carbonyl substitution reactions to afford [Mo(OAr)(S₂C₂R₂)₂]^{1–} and [Mo(CO)(QAr)(S₂C₂R₂)₂]^{1–} (Q = S, Se).²¹ The failure to expel both carbonyl groups is probably due to longer Mo–Q bond distances and attendant decreased steric interaction between carbonyl and thiolate or selenolate ligands. The synthesis of new Mo(IV) complexes on the basis of dicarbonyl precursors is outlined in Figure 2, together with yields. Phenolate complexes **1–3** and alkoxide complexes **4** and **5** are readily prepared in stoichiometric reactions. Monocarbonyl intermediates were not detected in the synthesis. Reaction of **5** with carbon monoxide indicates an equilibrium with this complex and [Mo(CO)(2-AdO)(S₂C₂Me₂)₂]^{1–} (ν_{CO} 1955 cm^{–1}), which is strongly disfavored. Axial ligands have been varied in **1–5** to examine their effects on oxo-transfer reaction rates.

Reaction of [Mo(CO)₂(S₂C₂Me₂)₂] with one equivalent of 2-AdS[–] or 2-AdSe[–] results in a color change from purple to green-brown, followed by development of a bright red-brown solution. By examining the reaction of **6** and **7** with carbon monoxide, it was shown that the green-brown chromophore is the intermediate [Mo(CO)(2-AdQ)(S₂C₂Me₂)₂]^{1–} (Q = S, ν_{CO} 1944 cm^{–1}; Q = Se, ν_{CO} 1952 cm^{–1}), which is similar to the monocarbonyls [Mo(CO)(QPh)(S₂C₂Me₂)₂]^{1–} (Q = S, Se), which have been isolated but not decarbonylated.²¹ For reasons not yet clear, the complexes [Mo(CO)(2-AdQ)(S₂C₂Me₂)₂]^{1–} are readily decarbonylated, whereas certain other species with large bulky ligands, such as [Mo(CO)(SeC₆H₂-2,4,6-Pr₃)(S₂C₂R₂)₂]^{1–}, are not.²¹ The structures of **2–7** are shown in Figures 3 and 4; selected metric data are collected in Tables 2 and 3. Together with previous data,^{19,21} the structural features of five-coordinate bis(dithiolene)Mo(IV) complexes are now well-established: square-pyramidal with mean Mo–S bond lengths of 2.31–2.33 Å, displacements δ of the molybdenum atom above the S₄ mean plane of 0.74–0.80 Å, dihedral angles θ between MS₂ chelate ring planes of 126–130°, and chelate ring C–C and C–S distances consistent with an endithiolate ligand oxidation state. The latter distances (Tables 2 and 3) may be compared to C=C, 1.33 Å; C–S, 1.75 Å; and C=S, 1.67 Å.³⁴ The axial Mo–O distances in **1–5** are somewhat variable (Table 2), being longest with the least basic ligand (C₆F₅O[–]) and shortest with the most basic ligands (Pr[–]O[–], 2-AdO[–]). Note that in the series [Mo(2-AdQ)(S₂C₂Me₂)₂]^{1–}, the Mo–Se bond distance in **7** is 0.60 Å longer than the Mo–O bond in **5**, providing a basis for relative carbonyl labilities in monocarbonyl intermediates. The absorption spectra of four oxygen-ligated complexes are compared in Figure 5 and those of **5–7**, in Figure

(34) Allen, F. H.; Kennard, O.; Watson, D. G.; Brammer, L.; Orpen, A. G.; Taylor, R. In *International Tables of Crystallography*; Wilson, A. J. C., Ed.; Kluwer Academic Publishers: Boston, 1995; Section 9.5.

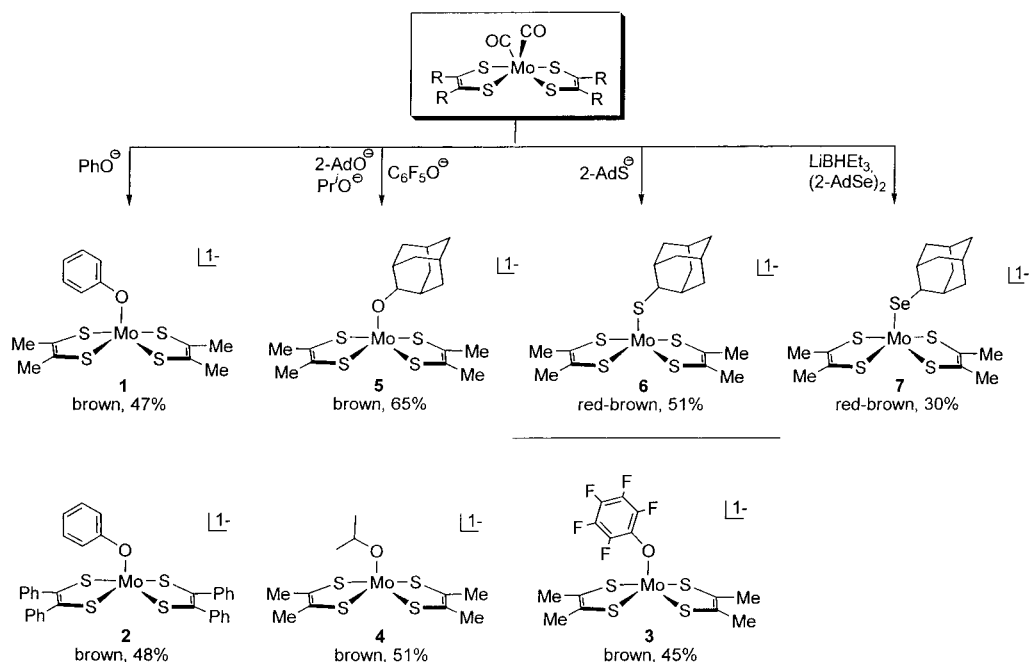


Figure 2. Scheme showing the synthesis of five-coordinate bis(dithiolene)Mo(IV) complexes 1–7.

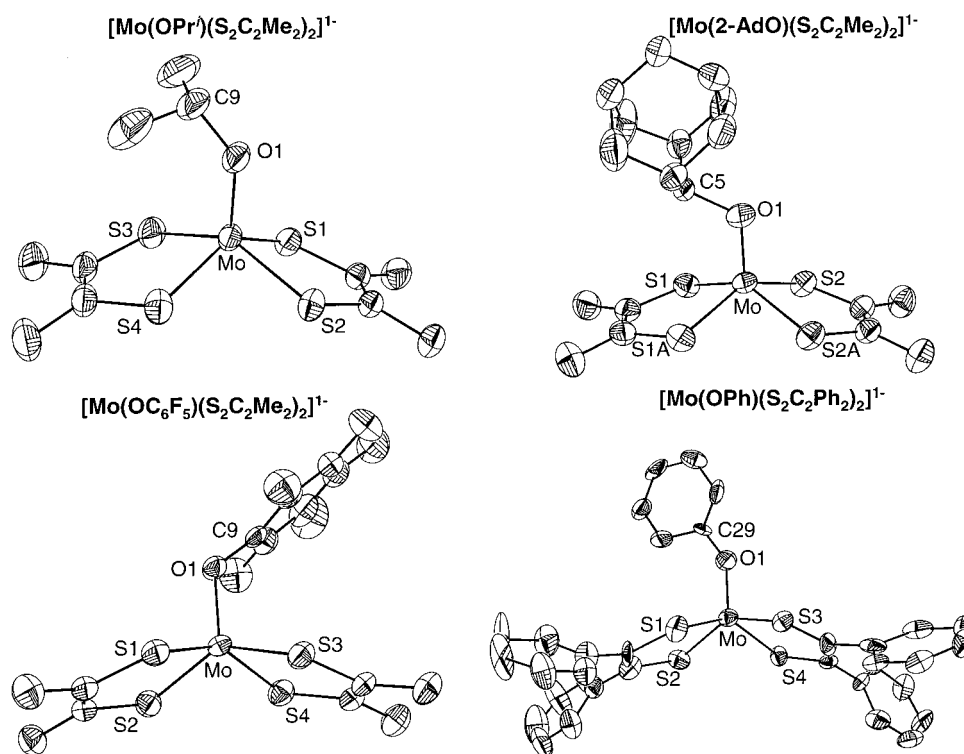


Figure 3. Structures of four complexes with axial anionic oxygen ligands— $[\text{Mo}(\text{OPr})(\text{S}_2\text{C}_2\text{Me}_2)_2]^{1-}$ and $[\text{Mo}(2\text{-AdO})(\text{S}_2\text{C}_2\text{Me}_2)_2]^{1-}$ (upper), and $[\text{Mo}(\text{OC}_6\text{F}_5)(\text{S}_2\text{C}_2\text{Me}_2)_2]^{1-}$, and $[\text{Mo}(\text{OPh})(\text{S}_2\text{C}_2\text{Ph}_2)_2]^{1-}$ (lower)—showing 50% probability ellipsoids and atom-labeling schemes. The major position of the three disordered sites of 2-adamantyl group in $[\text{Mo}(2\text{-AdO})(\text{S}_2\text{C}_2\text{Me}_2)_2]^{1-}$ is shown.

6. For at least the two highest energy features, the bands shift to the blue in the order $\text{Q} = \text{O} > \text{S} > \text{Se}$, indicating charge-transfer transitions involving the axial ligands. Brief comparisons with enzyme spectra have been made.²¹

The series $[\text{Mo}(2\text{-AdQ})(\text{S}_2\text{C}_2\text{Me}_2)_2]^{1-}$ ($\text{Q} = \text{O}, \text{S}, \text{Se}$) is the first in which axial ligands have been varied in the manner of reduced sites in the DMSOR enzyme family (Figure 1). Complexes **6** and **7** are intended as representatives of the sites of dissimilatory nitrate reductase and the Ser147Cys mutant of *Rs* DMSOR⁸ and of formate dehydrogenase, respectively.

Their reactivity properties will be described elsewhere. Complexes **1–5** are the closest approaches currently available to the five-coordinate site in DMSOR and possibly TMAOR. The oxo-transfer reactivity of this set of complexes is next considered.

Oxo Transfer Reactions and Kinetics. The reactions of three types of oxo-donor substrates $\text{XO} = \text{Se-oxide}, \text{N-oxide},$ and S-oxide were investigated. As will be seen, the final product in all three of the systems is the monooxo Mo(V) complex **9** or **10** arising from reaction sequence 1 in which the monooxo Mo-

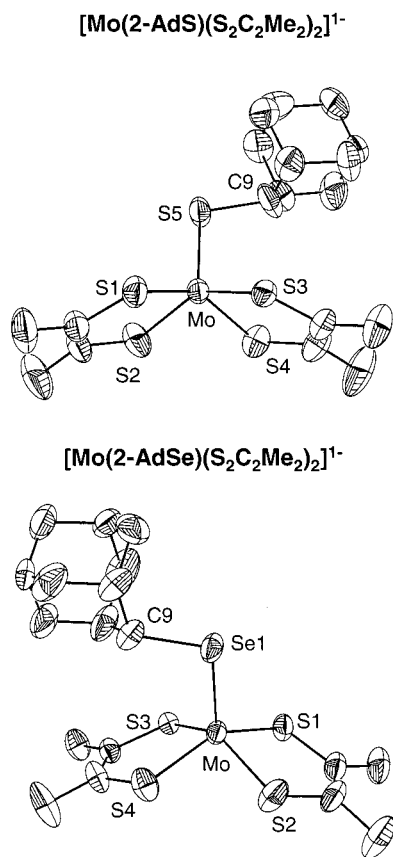
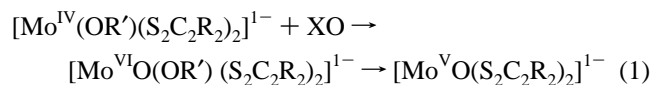
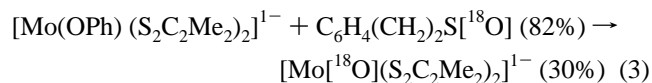
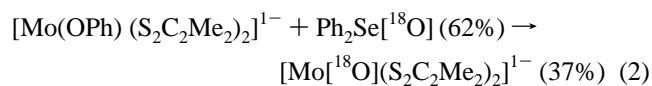


Figure 4. Structures of the complexes [Mo(2-AdS)(S₂C₂Me₂)₂]¹⁻ (upper) and [Mo(2-AdSe)(S₂C₂Me₂)₂]¹⁻ (lower) with axial thiolate and selenolate ligands, showing 50% probability ellipsoids and the atom-labeling schemes. The major positions of two disordered sites of 2-adamantyl groups are shown.

(VI) complex is formed by oxo transfer and decays to Mo(V). All of the reactions were carried out in acetonitrile solutions unless noted otherwise.



(a) Direct Atom Transfer. The first step in reaction sequence 1 was examined using two [¹⁸O]-labeled substrates in reactions, resulting in the conversions 2 and 3. Reaction 2 with 1.3 equivs of selenoxide proceeds to completion within several hours at room temperature. Because of the slow reactivity of sulfoxides

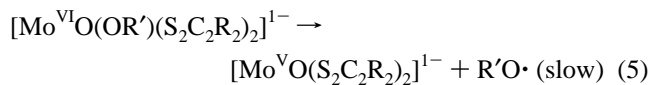
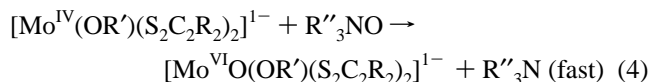


(vide infra), reaction 3 was conducted for 2 days at 50 °C with a large excess (84 equivs) of 2-thiaindane *S*-oxide. Earlier, we had demonstrated direct oxo transfer to a Mo^{IV}O center using Ph₂S[¹⁸O].³⁵ As in that experiment, some loss of label is observed upon workup of product because of trace water contamination and is probably abetted in reaction 3 by the forcing conditions that were used. We interpret these results in

(35) Schultz, B. E.; Gheller, S. F.; Muetterties, M. C.; Scott, M. J.; Holm, R. H. *J. Am. Chem. Soc.* **1993**, *115*, 2714–2722.

terms of direct (or primary³⁶) oxo-transfer reactions of all substrates XO examined in this work. In these and subsequent reactions, the blue-violet Mo^{VO} product is identified by its characteristic absorption spectrum and, on occasion, by its EPR spectrum with $\langle g \rangle = 1.996$ and $\langle a_{\text{Mo}} \rangle = 28.85$ G.

(b) *N*-oxides. Complexes **1–5** react with Me₃NO, although at varying rates. In solutions containing a 0.8–1.5 mM complex and 1.0 equiv of *N*-oxide, formation of the Mo^{VI}O complex in reaction sequence 1 is complete within 10 minutes for **1–3** and after ~25 min for **4**. For **5**, the reaction is 34% complete after 30 min; this relatively slow reaction is attributed to the steric effects of the 2-adamantyl group. The reaction mixtures change from brown (**1–5**) to green (typified by **8**), and over longer times to blue-violet (**9**) or green (**10**). The intervention of a Mo^{VI}O intermediate was demonstrated with **8**, whose tungsten analogue [WO(OPh)(S₂C₂Me₂)₂]¹⁻ is stable under oxo-transfer conditions.^{17,27b} This complex has a methyl resonance at 2.19 ppm and prominent absorption bands at 514 and 637 nm. When reaction 4, with complex **1** and Me₃NO as substrate, is monitored by ¹H NMR, signals appear at 2.11 (Me₃N) and 2.26 (Me) ppm. In the absorption spectrum, bands grow in at λ_{max} = 610 and 795 nm, red-shifted as compared to the bands of the tungsten complex. These spectral changes are entirely consistent with the formation of **8** which, despite numerous attempts, has not been isolated in pure form. Similar observations are made for reaction 4 involving **2–5**. The systems [Mo(OR')(S₂C₂Me₂)₂]¹⁻/Me₃NO (R' = Ph, Prⁱ, 2-Ad), when monitored spectrophotometrically after 16 h, show 90–94% conversion of **1**, **4**, or **5** to **9**. The ¹H NMR spectra clearly demonstrate the presence of phenol, 2-propanol, and 2-adamantanol. In reaction system 4, 83% of bound phenoxide appears as phenol by NMR integration. Thus, **8** and analogous complexes apparently decay by an internal redox process 5 in which a phenoxyl or alkoxy radical is developed and then quenched by capture of a hydrogen

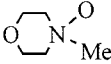
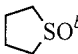
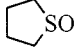
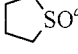
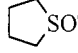


atom from solvent or trace water. Considerable difficulty was encountered in the earlier isolation of pure [Mo^{VI}O(OSiBu^tPh₂)-(bdt)₂]¹⁻, which is extremely sensitive hydrolytically.¹⁹ Indeed, complex **8** cannot be observed in situ unless the acetonitrile solvent is rigorously dry, and its decomposition to **9** is qualitatively more rapid in the presence of traces of water.

Reactions 4 with Me₃NO, *N*-methylmorpholine *N*-oxide, and (PhCH₂)₃NO were selected for kinetics study. With Me₃NO as a substrate, reactions of **2** and **3** are too rapid for convenient spectrophotometric measurements, and reactions of **4** and **5** sufficiently slow that in sequence 1, formation of **9** is competitive with oxo transfer. The time course of reaction 4 with Me₃NO is illustrated in Figure 7a. The intense absorption band of **1** at 345 decreases, and those at 610 and 795 nm of **8** grow in, as time increases. A tight isobestic point occurs at 372 nm, indicating that clean conversion of **1** to **8** without substantial accumulation of **9**. All reactions adhere to the second-order rate law 6. Kinetics data for *N*-oxide reduction reactions are presented in Table 4. Activation parameters were obtained from Eyring plots. The rate constants are ~10–200 M⁻¹ s⁻¹, with the slowest rate for the more hindered substrate.

(36) Holm, R. H. *Chem. Rev.* **1987**, *87*, 1401–1449.

Table 4. Rate Constants and Activation Parameters for Reactions 4 and 8

| | R' | R | XO | k_2^{298} (M ⁻¹ s ⁻¹) | ΔH^\ddagger (kcal/mol) | ΔS^\ddagger (eu) |
|---|-------------------------------|----|---|--|--------------------------------|--------------------------|
| 1 | Ph | Me | Me ₃ NO | 2.0(1) x 10 ² | 8.1(6) | -21(2) |
| 1 | Ph | Me |  | 1.8(1) x 10 ² | <i>a</i> | <i>a</i> |
| 1 | Ph | Me | (PhCH ₂) ₃ NO | 16(6) | 9.5(1) | -21(1) |
| 1 | Ph | Me |  | 1.5(2) x 10 ⁻⁴ | 10.1(4) | -39(1) |
| 1 | Ph | Me | Me ₂ SO ^b | 1.3 x 10 ^{-6 c} | 14.8(5) | -36(1) |
| 2 | Ph | Ph |  | 3.4(2) x 10 ⁻⁴ | <i>a</i> | <i>a</i> |
| 3 | C ₆ F ₅ | Me |  | 5.2(2) x 10 ⁻³ | 11.8(3) | -30(5) |
| 4 | Pr ⁱ | Me |  | 5(1) x 10 ⁻⁶ | <i>a</i> | <i>a</i> |

^a Not measured. ^b Ref 17. ^c Calculated value from the Eyring equation. ^d Measured in THF. ^e Measured in neat substrate.

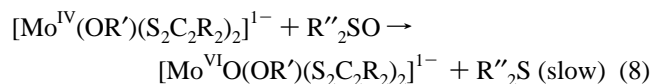
The negative entropies of activation indicate an associative transition state consistent with a second-order reaction. The conversion **8** → **9** is illustrated in Figure 7b. The 610-nm feature

$$-d[\text{Mo}^{\text{IV}}]/dt = k_2[\text{Mo}^{\text{IV}}][\text{XO}] \quad (6)$$

$$-d[\text{Mo}^{\text{VI}}\text{O}]/dt = k_1[\text{Mo}^{\text{VI}}\text{O}] \quad (7)$$

of **8** decreases in intensity as the 830 nm band of **9** increases. The final spectrum is that of **9** measured separately. The reaction follows first-order rate law 7. The observed rate constants $k_1/[\text{Mo}^{\text{VI}}\text{O}]_0 \approx 0.087\text{--}0.10 \text{ M}^{-1} \text{ s}^{-1}$ at ambient temperature are smaller than k_2 , thereby allowing both steps in sequence 1 to be examined separately and accounting for the isosbestic points in Figure 7.

(c) **S-oxides.** In reaction sequence 1, the relative rates of the two steps are reversed, as compared to reactions with *N*-oxides. Oxo-transfer reaction 8 is quite slow, even in neat DMSO or tetramethylene *S*-oxide (TMSO), and reaction 5 is fast. Consequently, the appearance of only the Mo^{VO} product is measurable by spectrophotometry or EPR. In reaction 8 with complex **1** tetramethylene sulfide was detected by gas chroma-



tography, thereby supplying additional evidence for direct oxo transfer, and phenol was formed quantitatively. Complexes **2–4** also react with DMSO and TMSO. The reactions of complex **5** were very sluggish, owing to the steric bulk of the adamantyl group, and were not pursued. Spectrophotometric monitoring of reaction 8 with **1** and TMSO is shown in Figure 8. Over time, absorption bands of **1** at 345, 396, and 475 nm decrease in intensity, but those of **9** at 579 and 830 nm increase. A sharp isosbestic point at 552 nm indicates no appreciable build-up of intermediate **8**.

Rate constants and activation parameters for reaction 8 are collected in Table 4. The rate constants $k_2 \approx 10^{-3}\text{--}10^{-6} \text{ M}^{-1}$

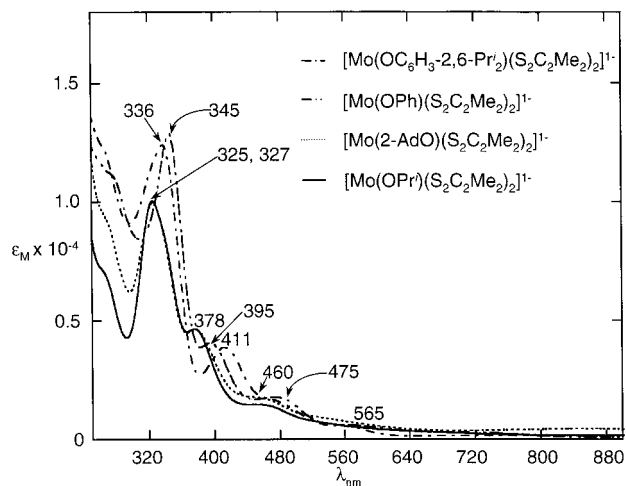


Figure 5. UV/vis spectra of [Mo(OC₆H₃Prⁱ₂)(S₂C₂Me₂)₂]¹⁻ (- · -), [Mo(OPh)(S₂C₂Me₂)₂]¹⁻ (···), [Mo(OPr)(S₂C₂Me₂)₂]¹⁻ (·····), and [Mo(2-AdO)(S₂C₂Me₂)₂]¹⁻ (—) in acetonitrile; selected band maxima are indicated.

s⁻¹, are small compared to the values $k_1/[\text{Mo}^{\text{VI}}\text{O}]_0 \approx 0.089\text{--}0.31 \text{ M}^{-1} \text{ s}^{-1}$, supporting analysis of the data in terms of rate law 6. The large negative entropies of activation again indicate an associative mechanism. The rate constant ratio $k_2^{\text{TMSO}}/k_2^{\text{DMSO}} \approx 115$ for reactions of **1** must arise from the less hindered nature of TMSO in binding to molybdenum in the associative transition state. Because of its increased reaction rate, TMSO was used as substrate in all of the other reactions. Reduction of the basicity of the dithiolene ligands by substitution of phenyl for methyl has little effect on reaction rates; with TMSO as substrate, $k_2(\mathbf{2})/k_2(\mathbf{1}) = 2.3$. Variation of axial ligands increases the rate constant in the order C₆F₅ > Ph ≫ Prⁱ. To achieve an appreciable rate for **4**, its reaction was measured in neat TMSO. Although not strictly comparable to other values, the rate constant is a factor of 300 smaller than the value for **1** with the same substrate.

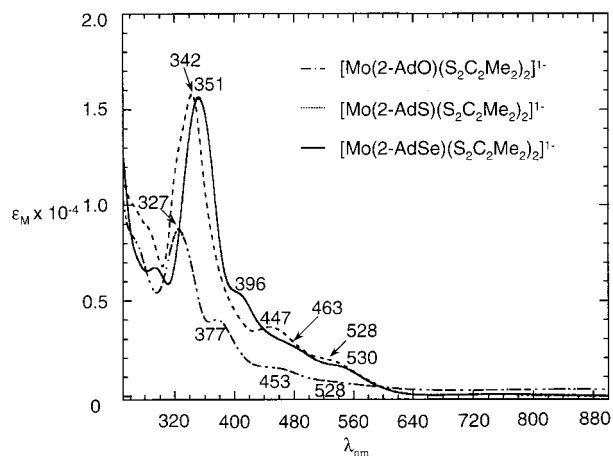


Figure 6. UV/vis spectra of $[\text{Mo}(2\text{-AdO})(\text{S}_2\text{C}_2\text{Me}_2)_2]^{1-}$ (---), $[\text{Mo}(2\text{-AdS})(\text{S}_2\text{C}_2\text{Me}_2)_2]^{1-}$ (.....), and $[\text{Mo}(2\text{-AdSe})(\text{S}_2\text{C}_2\text{Me}_2)_2]^{1-}$ (—) in acetonitrile; selected band maxima are indicated.

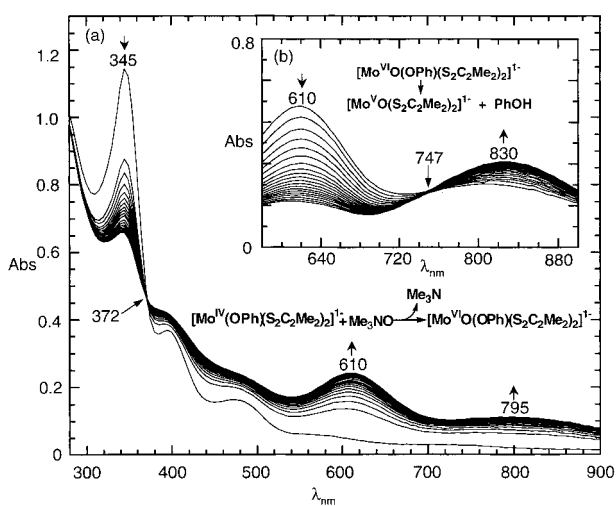
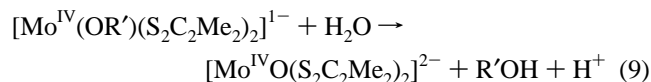


Figure 7. Spectrophotometric monitoring of reactions: (a) the system $[\text{Mo}^{\text{IV}}(\text{OPh})(\text{S}_2\text{C}_2\text{Me}_2)_2]^{1-} + \text{Me}_3\text{NO} \rightarrow [\text{Mo}^{\text{VI}}\text{O}(\text{OPh})(\text{S}_2\text{C}_2\text{Me}_2)_2]^{1-}$ initially containing 0.744 mM $[\text{Mo}^{\text{IV}}(\text{OPh})(\text{S}_2\text{C}_2\text{Me}_2)_2]^{1-}$ and 0.818 mM Me_3NO in acetonitrile at room temperature; (b) the conversion of $[\text{Mo}^{\text{VI}}\text{O}(\text{OPh})(\text{S}_2\text{C}_2\text{Me}_2)_2]^{1-}$ to $[\text{Mo}^{\text{VO}}(\text{S}_2\text{C}_2\text{Me}_2)_2]^{1-}$ in a system initially containing 1.39 mM $[\text{Mo}^{\text{IV}}(\text{OPh})(\text{S}_2\text{C}_2\text{Me}_2)_2]^{1-}$ and 1.45 mM Me_3NO in acetonitrile at room temperature.

(d) Hydrolysis. We have emphasized the instability of **8** to internal redox reaction 5 and to traces of water. The initial hydrolysis product preceding formation of **9** has not been identified. Complexes **1–5** are also highly sensitive to water. Even under conditions intended to be rigorously dry, reaction 9 can proceed, resulting in the formation of $\text{Mo}^{\text{IV}}\text{O}$ complexes. One of these, orange-brown **11**, has been isolated and structurally characterized.²¹ To differentiate kinetically hydrolysis from oxo transfer, the reactions of **1** and **4** with water have been investigated kinetically under pseudo-first-order conditions in acetonitrile solutions. The reactions, monitored spectrophotometrically (not shown), proceed with well-defined isosbestic points and were treated as second-order within the water concentration range employed. The final spectra are that of **11** measured separately.²¹ Rates constants are the same for **1** and **4** and are given in Table 5. The modest isotope effect $k_2^{\text{H}}/k_2^{\text{D}}$



metrically (not shown), proceed with well-defined isosbestic points and were treated as second-order within the water concentration range employed. The final spectra are that of **11** measured separately.²¹ Rates constants are the same for **1** and **4** and are given in Table 5. The modest isotope effect $k_2^{\text{H}}/k_2^{\text{D}}$

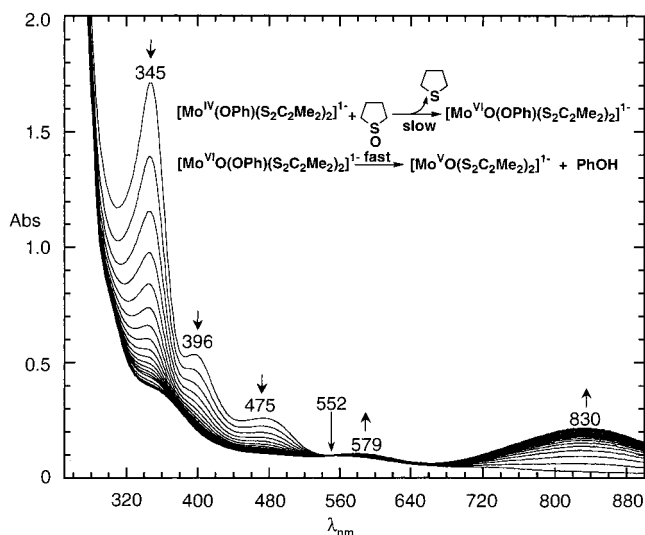


Figure 8. UV/vis spectra for the reaction $[\text{Mo}^{\text{IV}}(\text{OPh})(\text{S}_2\text{C}_2\text{Me}_2)_2]^{1-} + (\text{CH}_2)_4\text{SO} \rightarrow [\text{Mo}^{\text{VI}}\text{O}(\text{OPh})(\text{S}_2\text{C}_2\text{Me}_2)_2]^{1-} + (\text{CH}_2)_4\text{S}$ (slow) followed by the reaction $[\text{Mo}^{\text{VI}}\text{O}(\text{OPh})(\text{S}_2\text{C}_2\text{Me}_2)_2]^{1-} \rightarrow [\text{Mo}^{\text{VO}}(\text{S}_2\text{C}_2\text{Me}_2)_2]^{1-} + \text{PhOH}$ (fast) at room temperature. The system contained initially 1.05 mM $[\text{Mo}^{\text{IV}}(\text{OPh})(\text{S}_2\text{C}_2\text{Me}_2)_2]^{1-}$ and 2.69 M $(\text{CH}_2)_4\text{SO}$.

Table 5. Kinetics and Activation Parameters for Reaction 9

| R' | | k_2^{298} ($\text{M}^{-1} \text{s}^{-1}$) | ΔH^\ddagger (kcal/mol) | ΔS^\ddagger (eu) |
|-----------------|----------------------|---|--------------------------------|--------------------------|
| Ph | H_2O | $1.2(2) \times 10^{-2}$ | 10.0(2) | -34(1) |
| | D_2O | $4.7(1) \times 10^{-3}$ | <i>a</i> | <i>a</i> |
| Pr ⁱ | H_2O | $1.1(1) \times 10^{-2}$ | 10.6(4) | -32(1) |

^a Not measured.

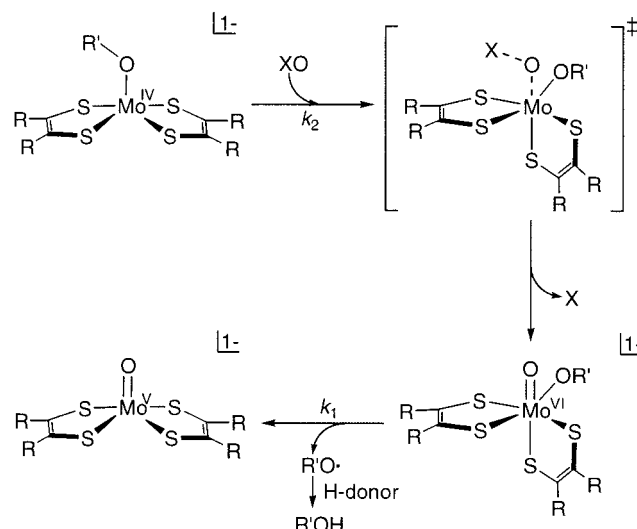


Figure 9. Summary of the oxo-transfer analogue reaction systems based on $[\text{Mo}^{\text{IV}}(\text{OR}')(\text{S}_2\text{C}_2\text{R}_2)_2]^{1-}$ ($\text{XO} = \text{N-oxide}, \text{S-oxide}$), including the conversion of the $\text{Mo}^{\text{VI}}\text{O}$ intermediate to the Mo^{VO} final product.

$= 2.6$ indicates that outright O–H bond dissociation is not involved in the rate-determining step. With complex **1**, reaction 9 is $\sim 10^4$ slower than oxo transfer from Me_3NO . It is, however, $\sim 10^2\text{--}10^4$ faster than oxo transfer from *S*-oxides, emphasizing the requirement for anhydrous conditions when studying reaction 8.

(e) Mechanistic Aspects. Reaction sequence 1 is summarized in Figure 9. We assume the structure of the $\text{Mo}^{\text{VI}}\text{O}$ intermediate as being the same as $[\text{WO}(\text{OPh})(\text{S}_2\text{C}_2\text{Me}_2)_2]^{1-}$, which has been isolated and structurally characterized.^{17,27b} Reactions of **1** and related complexes with *N*-oxides and *S*-oxides share the

common features of second-order kinetics, associative transition states, and appreciable enthalpies of activation (8–15 kcal/mol). These features are anticipated in earlier molybdenum oxo-transfer systems,^{35–40} developed prior to proof of pterin-dithiolene ligand binding to molybdenum. All utilize the minimal reaction $\text{Mo}^{\text{IV}}\text{O} + \text{XO} \rightarrow \text{Mo}^{\text{V}}\text{O}_2 + \text{X}$, not yet known to be a physiological process, involving complexes with sulfur ligands but not dithiolenes. Of these systems, that based on the complex $[\text{Mo}^{\text{IV}}\text{O}(\text{Bu}^t\text{L-NS}_2)_2]$ is the most thoroughly analyzed.³⁸ Certain considerations raised in that work apply here.

Reaction rates are highly substrate-dependent, with k_2 values spanning a range of 10^8 . For the five reactions whose activation parameters were determined, $T|\Delta S^\ddagger|$ is 40–53% of ΔG^\ddagger . Activation free energies are, therefore, not dominated by enthalpic contributions, but two such contributions are indicated by relative rates. The much faster reactions of *N*-oxides than *S*-oxides correlate with two substrate properties, gas-phase bond dissociation energies and basicities. For Me_3NO , $D(\text{N}-\text{O}) = 61$ kcal/mol has been obtained from calorimetric data,⁴¹ and 71 kcal/mol from a combination of calorimetric and computational results.⁴² For DMSO and TMSO, $D(\text{S}-\text{O}) = 87$ kcal/mol from thermodynamic data⁴³ and 86 kcal/mol by computation,⁴⁴ respectively. The gas-phase proton affinity of Me_3NO (235 kcal/mol) is substantially larger than that of DMSO (211 kcal/mol).⁴⁵ Also, Me_3NO is a stronger base in aqueous solution ($\text{p}K_{\text{BH}}^a$, 4.6)⁴⁶ than is DMSO ($\text{p}K_{\text{BH}}^a$, -1.8)⁴⁷ and TMSO ($\text{p}K_{\text{BH}}^a$, -1.3).⁴⁸ although these results were not all obtained by the same procedure. Thus, the fast rates of reaction of substrate XO are associated with weaker X–O bonds and higher basicity. Further, the fastest rate of TMSO reduction is found with **3**, which carries the most electronegative axial ligand, a feature that should promote substrate binding. We infer a concerted transition state involving both X–O bond-weakening and Mo–O bond-making with concomitant structural rearrangement to a configuration approaching that of the $\text{Mo}^{\text{V}}\text{O}$ intermediate. The structure of the latter (e.g., **8**) may be safely assumed to be that of $[\text{WO}(\text{OPh})(\text{S}_2\text{C}_2\text{Me}_2)_2]^{1-}$, which has a distorted *cis*-octahedral stereochemistry.^{17,27b} The mechanism of oxo transfer will be considered in more detail in a future report on the reactivity of $[\text{W}^{\text{IV}}(\text{OR}')(\text{S}_2\text{C}_2\text{R}_2)]^{1-}$ complexes, which have been examined with a wider range of substrates.^{27b} The $\text{W}^{\text{V}}\text{O}$ products are stable, thereby obviating the last step in the reaction scheme for molybdenum complexes (Figure 9).

Relation to Enzymes. This work provides the first analogue reaction systems for reduction of biologically relevant *N*-oxide and *S*-oxide substrates by desoxo bis(dithiolene)-Mo(IV) complexes with axial ligands that simulate serinate coordinate in *Rs* DMSOR (Figure 1). The steps of substrate binding and reduction by oxo transfer doubtless occur in the enzyme, as shown for *Rc* DMSOR,⁴⁹ and the transition state for oxo transfer from substrate may have characteristics in common with the analogue systems. Thereafter, interesting differences are evident, albeit from a limited enzyme reactivity database.^{23,49–51} First,

DMSORs reduce both DMSO and Me_3NO ,⁴⁹ as exemplified by *Ec* DMSOR,⁵⁰ whereas TMAORs such as the *Ec* enzyme reduce *N*-oxides but do not reduce *S*-oxides, including DMSO and TMSO, at a detectable rate.²³ As shown here, *complex 1* is intrinsically competent to reduce both substrate types, although at widely different rates (Table 4). Second, rates of analogue systems and enzymes are markedly different. Second-order rate constants under single-turnover conditions are unavailable for enzyme systems. For comparison to enzymes, recourse is taken to $k_{\text{cat}}/K_{\text{M}}$ values, which are effectively second-order rate constants for substrate reduction under steady state (Michaelis–Menten) conditions. The following values have been reported for the indicated substrates: *Ec* DMSOR, DMSO, $1.9 \times 10^6 \text{ M}^{-1} \text{ s}^{-1}$;^{50,52} *Ec* TMAOR, Me_3NO , $2.2 \times 10^6 \text{ M}^{-1} \text{ s}^{-1}$;²³ *Sm* TMAOR, Me_3NO , $7.1 \times 10^6 \text{ M}^{-1} \text{ s}^{-1}$.⁵¹

Although comparison among enzymes and between enzymes and analogue systems is obviously inexact, the conclusion is inescapable that, in terms of second-order rate constants, the reduced enzymes in *in vitro*-reconstituted systems are orders of magnitude more reactive than Mo(IV) complexes such as **1**. Under steady-state conditions, all steps in a catalytic cycle proceed at the same rate but not necessarily with the same rate constant. There is little information on which step—substrate binding, oxygen atom transfer from substrate to the molybdenum center, product release, or proton-coupled electron transfer—controls the turnover rate of an enzyme. In an *Rc* DMSOR system, formation of an enzyme–substrate complex is rate-limiting at pH 5.5, whereas at pH 8.0, the oxo-transfer step is limiting.⁴⁹ Tight binding of both pterin dithiolene ligands and serinate to molybdenum during the catalytic cycle of *Rs* DMSOR is supported by resonance Raman spectra.⁵³ We have no reason to believe that the corresponding metal–ligand binding does not obtain in the analogue reaction systems. However, it is appropriate to note several of the many real or possible differences between analogue and enzyme systems. The enzymes possess a crevice or “funnel”,^{5,9–11,14} apparently for efficacious passage of substrate from the enzyme surface and binding at the catalytic site,⁵ a probable rate-enhancing feature. The molybdenum cofactor is held in the protein structure by a large number of hydrogen bonds involving the pterin nucleus and phosphate-nucleotide side chains. These interactions, adjacent residues, and any protein-induced structural features presumably condition the active site in a manner favorable to oxo transfer. The $[\text{Mo}^{\text{V}}\text{O}(\text{O}\cdot\text{Ser})(\text{S}_2\text{pd})_2]$ site in oxidized *Rs* DMSOR is described by Li et al.⁶ as a distorted trigonal prism, whereas the tungsten analogue of **8** is closer to the octahedral limit. Possibly, the trigonal prismatic structure is influenced by the protein and is nearer to the transition state geometry for

(44) Jenks, W. S.; Matsunaga, N.; Gordon, M. *J. Org. Chem.* **1996**, *61*, 1275–1283.

(45) Hunter, E. P. L.; Lias, S. G. *J. Phys. Chem. Ref. Data* **1998**, *27*, 413–656, and references therein.

(46) Nylén, P. Z. *Anorg. Allg. Chem.* **1941**, *246*, 227–330.

(47) Landini, D.; Modena, G.; Scorrano, G.; Taddei, F. *J. Am. Chem. Soc.* **1969**, *91*, 6703–6707.

(48) Curci, R.; Di Furia, F.; Levi, A.; Lucchini, V.; Scorrano, G. *J. Chem. Soc., Perkin II* **1975**, 341–344.

(49) Adams, B.; Smith, A. T.; Bailey, S.; McEwan, A. G.; Bray, R. C. *Biochemistry* **1999**, *38*, 8501–8511.

(50) Simala-Grant, J. L.; Weiner, J. H. *Eur. J. Biochem.* **1998**, *251*, 510–515, and references therein.

(51) Santos, J.-P. D.; Iobbi-Nivol, C.; Couillant, C.; Giordano, G.; Méjean, V. *J. Mol. Biol.* **1998**, *284*, 421–433.

(52) We previously misquoted the second-order rate constant for oxidation of Me_2S -reduced DMSOR by DMSO as $4.3 \times 10^2 \text{ M}^{-1} \text{ s}^{-1}$;¹⁷ This value is the binding constant of substrate to reduced enzyme;⁴⁹ the value of $k_{\text{cat}}/K_{\text{M}}$ apparently has not been determined.

(53) Garton, S. D.; Hilton, J.; Oku, H.; Crouse, B. R.; Rajagopalan, K. V.; Johnson, M. K. *J. Am. Chem. Soc.* **1997**, *119*, 12906–12916.

(37) Holm, R. H. *Coord. Chem. Rev.* **1990**, *100*, 183–221.

(38) Schultz, B. E.; Holm, R. H. *Inorg. Chem.* **1993**, *32*, 4244–4248.

(39) Enemark, J. H.; Young, C. G. *Adv. Inorg. Chem.* **1994**, *40*, 1–88.

(40) Laughlin, L. J.; Young, C. G. *Inorg. Chem.* **1996**, *35*, 1050–1058.

(41) Acree, W. E., Jr.; Tucker, S. A.; Ribeiro da Silva, M. D. M. C.; Matos, A. R.; Gonçalves, J. M.; Ribeiro da Silva, M. A. V. *J. Chem. Thermodyn.* **1995**, *27*, 391–398.

(42) Haaland, A.; Thomassen, H.; Stenström, Y. *J. Mol. Struct.* **1991**, *263*, 299–310.

(43) Donahue, J. P.; Holm, R. H. *Polyhedron* **1993**, *12*, 571–589.

oxo transfer. In a reaction sequence such as that in Figure 9, a relatively electron-deficient Mo(IV) center is expected to enhance substrate binding, but a relatively electron-rich center should promote formation of the Mo^{VI}O state by oxo transfer. As shown previously, dithiolene ligands by virtue of Mo–S bond covalency can act as an “electronic buffer” to maintain charge distribution at the molybdenum center as other ligands are varied or the oxidation state is changed.⁵⁴ In one set of oxomolybdenum complexes containing a dithiolene ligand, Mo^{VO}/Mo^{IVO} redox potentials are linearly related to calculated charges per sulfur atom.⁵⁵ The latter are dependent on the dithiolene itself. The buffer effect can exist in both analogue and enzyme, but ligand structural and environmental effects in the latter could render the buffered charge distribution more favorable to the rate-limiting step in oxo transfer, as compared to analogues, which are simplified to the point of

(54) Westcott, B. L.; Gruhn, N. E.; Enemark, J. H. *J. Am. Chem. Soc.* **1998**, *120*, 3382–3386.

(55) Helton, M. E.; Gruhn, N. E.; McNaughton, R. L.; Kirk, M. L. *Inorg. Chem.* **2000**, *39*, 2273–2278.

lacking structure beyond the chelate rings. Last, complexes such as **1** are not represented here as highly accurate analogues of the reduced sites of DMSOR and TMAOR. They are, however, the nearest approaches currently available and provide the basis for further evolution of analogue complexes that more closely approximate the reaction rates of enzyme sites.

Acknowledgment. This research was supported by NSF Grant CHE 98-76457. We thank K.-M. Sung for valuable discussions, Prof. H. Schindelin for access to ref. 6 prior to publication, and Prof. E. N. Jacobsen for use of a gas chromatograph.

Supporting Information Available: Crystallographic data for the compounds in Tables 1 and 2 and selected Eyring plots for reactions 8 and 9 (PDF). This material is available free of charge via the Internet at <http://pubs.acs.org>.

JA003546U